12-15-2010

An Adaptive Coverage Control Algorithm for Deployment of Nonholonomic Mobile Sensors

Chaouki T. Abdallah

Jose Marcio Luna

Rafael Fierro

John Wood

49th IEEE Conference on Decision and Control
December 15-17, 2010
Hilton Atlanta Hotel, Atlanta, GA, USA

An Adaptive Coverage Control Algorithm for Deployment of Nonholonomic Mobile Sensors

Jose-Marcio Luna, Rafael Fierro, Chaouki Abdallah and John Wood

Abstract— **We show the Lyapunov stability and convergence of an adaptive and decentralized coverage control for a team of mobile sensors. This new approach assumes nonholonomic sensors rather than the usual holonomic sensors found in the literature. The kinematics of the unicycle model and a nonlinear control law in polar coordinates are used in order to prove the stability of the controller applied over a team of mobile sensors. The convergence and feasibility of the coverage control algorithm are verified through simulations in Matlab. Furthermore, some experiments are carried out using a team of four Pioneer 3-AT robots sensing a piecewise constant light distribution function.**

I. Introduction

Literature related to oil spills [1] and forest fires [2] shows that some systems present motion dynamics that make them more complicated to overcome without putting humans in danger. Currently, the use of manned aerial vehicles for firefighting requires skillful enough pilots to avoid crashing in the attempt to put out a fire. Moreover, firefighters must get a qualitative estimation of the fire dynamics almost by direct observation. In another scenario, Cortez *et al.,* exposed in [3] that building radiation maps involving nuclear material are still done using people for taking measurements close to the radiated area.

Coverage controllers become promising with the latest developments on wireless communications, material science, new sensors and the constant improvement of computational power. The possibilities to send small unmanned aerial, terrestrial or underwater vehicles which coordinate actions to sense and map an area of interest are increasing as the research in decentralized algorithms and hardware progresses.

In the field of sensory coverage there are several problem dependent approaches such as the one described by Choset in [4], the strategy to build radiation maps presented by Cortez *et al.,* in [5] or the reconfigurable sensor array in a gradient climbing mission explained by Ögren in [6]. Some approaches use centroidal Voronoi Tessellations as the equitable partition policies dividing the workspace in sub-regions explained by Pavone *et al.,* [7]; the on-line task allocation based on local information presented by Fu *et al.,* [8] and the local coverage optimization considering the sensory radius of a team of agents formulated by Stergiopoulos *et al.,* [9].

Based on [10], the coverage control problem is associated to a cost function which determines a problem-dependent metric of the coverage performance. It is possible to implement a controller to determine the *optimal placement* of the sensors in an environment. Lee *et al.,* present in [11] an approach of coverage control with environmental sensing where a team of robots should position themselves over an area such that they concentrate themselves in the area with the greatest amount of a chemical using an adaptive triangular mesh. In [12] Schwager *et al.,* propose an optimization criterion to distribute a team of hovering robots with downward facing cameras to obtain the best view of an environment. The authors propose a metric based on the minimum information per pixel in order to elaborate the cost function.

Because of the complexity found in the analysis of networks of dynamic systems, it is common to consider simple dynamical models such as the single integrator [13], or the double and higher order integrators [14]. Recently, Kwok and Martinez in [15] have used a hybrid system approach to attack the decentralized control problem described in [13] using nonholonomic sensors. The authors model the problem as a hybrid automaton with a set of states implementing some motion behaviors in a team of unicycle agents with fixed and variable forward velocity. The agents are assumed to have a previous knowledge of the sampling space.

A. Contributions

Our work is motivated by the one presented by Schwager *et al.,* in [16] where the authors describe the development of an adaptive coverage control for mobile sensor networks and provide the stability analysis of the controller. The authors assume that the mobile sensors do not have nonholonomic constraints and that the estimated density function is static. However, several real world vehicles such as aircrafts at cruising attitude, sea vessels and skid-steered mobile robots have nonholonomic constraints.

Calculations associated to Voronoi partitions and their centers of mass may require a considerable computational cost, but the analysis of this feature is out of the scope of this paper. In this work, we use a Voronoi partition approach given the availability of software libraries such as Voro++ [17] for C++, some Matlab functions and well known implementation techniques based on previous literature [3], [7], [8].

The performance of the results given for holonomic mobile sensors can be severely affected or even invalidated [15], when they are adapted to nonholonomic mobile sensors. In this specific scenario, the control law designed for a holonomic vehicle given by the single integrator [3] does not work for a nonholonomic vehicle defined by the unicycle

J. Luna, R. Fierro and C. T. Abdallah are with the Department of Electrical & Computer Engineering, The University of New Mexico, Albuquerque, NM 87131-0001, USA {jmarcio,rfierro,chaouki}@ece.unm.edu

J. Wood is with the Department of Mechanical Engineering, The University of New Mexico, Albuquerque, NM 87131-0001, USA jw@unm.edu

vehicle. Our main goal in this work is to provide the necessary mathematical background to use nonholonomic mobile sensors along with the adaptive coverage control presented in [16], and guarantee the stability of the system.

The paper is organized as follows: Section II shows the mathematical background related to Voronoi partitions and locational optimization and the adaptive coverage control for holonomic sensor networks which inspired this work. In Section III, we present our main theoretical result which shows the stability of the adaptive coverage control for nonholonomic sensor networks. Section IV shows simulation results obtained by using Matlab. Section V illustrates the experimental results obtained by using a team of four Pioneer 3-AT robots sensing a dynamic light distribution. Lastly, Section VI summarizes the main conclusions and limitations of our approach as well as future work to overcome those limitations.

II. Mathematical Background

Voronoi partitions are a typical feature of several biological systems [18] and recently they have received special attention for their application in disciplines such as cellular biology, image compression, statistics and robotics among. Before any further discussion, let us start with some necessary definitions.

A. Voronoi Diagrams

We based the following definition on the one in [18]

Definition 1: Given an open set $Q \subseteq \mathbb{R}^N$, the set $\{V_i\}_{i=1}^k$ is called a Voronoi tesselation or diagram of Q if $V_i \cap V_j = \emptyset$ for $i \neq j$ and $\bigcup_{i=1}^k V_i = Q$. Given a set of points $\{p_i\}_{i=1}^k$ belonging to Q, the Voronoi region V_i corresponding to the point p_i is defined by

$$\begin{aligned} V_i &= \{x \in Q \mid \|x - p_i\| < \|x - p_j\| \\ &\quad \text{for } i, j = 1, \ldots, k, j \neq i\}. \end{aligned}$$

Where $\|\cdot\|$ denote the Euclidean norm on $\mathbb{R}^N$. The points $\{p_i\}_{i=1}^k$ are called *generator points*, and V_i is the *Voronoi region* associated to the generator point p_i.

B. Locational Optimization

Based on [19], let $Q \subset \mathbb{R}^N$ be a convex polytope including its interior. Assume a mapping $\phi(q) : Q \mapsto \mathbb{R}_+$ with $q \in Q$ called a *distribution density function* (or *sensory function*) which represents a measurement of the probability of a specific event on Q. The locational optimization function is then defined as

$$\mathcal{H}_V(P) = \sum_{i=1}^{n} \int_{V_i} f(\|q - p_i\|)\phi(q)dq, \tag{1}$$

where P is the set of all the n generator points $\{p_1, \ldots, p_n\} \in Q$ and V_i is the Voronoi partition of the i-th robot.

Now, based on [13] we can adapt some physical concepts namely, the mass M_{V_i}, the first moment L_{V_i}, the polar moment of inertia $J_{V,p}$ and the centroid C_{V_i} of a Voronoi region V_i. Their definitions are given by the following equations,

$$\begin{aligned} M_{V_i} &= \int_{V_i} \phi(q)dq, \\ L_{V_i} &= \int_{V_i} q\phi(q)dq, \\ J_{V,p} &= \int_{V_i} \|q - p_i\|^2 \phi(q)dq, \\ C_{V_i} &= \frac{1}{M_{V_i}} \int_{V_i} q\phi(q)dq. \end{aligned} \tag{2}$$

From [13], if we define $f(\|q - p_i\|) = \|q - p_i\|^2$ and replace it in (1), after applying a partial derivative with respect to p_i we have that

$$\begin{aligned} \frac{\partial \mathcal{H}_V(P)}{\partial p_i} &= \int_{V_i} \frac{\partial}{\partial p_i} f(\|q - p_i\|)\phi(q)dq \\ &= 2M_{V_i}(p_i - C_{V_i}). \end{aligned} \tag{3}$$

Therefore, all the Voronoi tessellations in Q where the generator points are at the same time the centroids of their Voronoi partitions minimize the locational optimization function. These tessellations are usually called *centroidal Voronoi tessellations* [18].

C. Adaptive Control for Holonomic Sensors

In [16] the authors propose an approach which guarantees that the network of mobile agents minimizes the cost function $\mathcal{H}_V(P)$ in (1). They assume that each agent measures the sensory function without requiring a previous knowledge.

In order to deal with the lack of knowledge of the sampling space they proposed a decentralized adaptive control based on the following assumptions,

Assumption 1 (Matching Conditions): There exists a parameter vector $a \in \mathbb{R}_+^m$ and a vector function $\mathcal{K} : Q \mapsto \mathbb{R}_+^m$ such that

$$\phi(q) = \mathcal{K}(q)^T a, \tag{4}$$

where $m \in \mathbb{N}$, and $(\cdot)^T$ denotes transpose.

The parameter vector a is unknown by the agents but $\mathcal{K}(q)$ is available to them.

Assumption 2 (Lower Bound): Given that $a(j)$ is the j-th element of the vector a and $\beta \in \mathbb{R}_+$ then

$$a(j) \geq \beta \quad \forall j = 1, \ldots, m,$$

The reason for a lower bound for the parameter vector $a(j)$ is to avoid that $\mathcal{K}(q)^T a = \phi(q) = 0$ leading to a zero in the denominator of (2).

The sensory function estimated by the i-th agent is given by $\hat{\phi}_i = \mathcal{K}(q)^T \hat{a}_i$, where $\hat{a}_i$ is the estimation of the parameter vector a calculated by the agent i. Furthermore the parameter error vector $\tilde{a}_i$ is given by

$$\tilde{a}_i = \hat{a}_i - a_i. \tag{5}$$

In [13] the mobile agents are considered holonomic vehicles with first-order continuous dynamics, that is

$$\dot{p}_i = u_i. \tag{6}$$

The control law is defined as

$$u_i = k(\hat{C}_{V_i} - p_i), \tag{7}$$

where $\hat{C}_{V_i}$ is an estimate of the real centroid C_{V_i} of the i-th Voronoi region defined by

$$\hat{C}_{V_i} = \frac{\hat{L}_{V_i}}{\hat{M}_{V_i}} = \frac{\int_{V_i} q\hat{\phi}(q)dq}{\int_{V_i} \hat{\phi}(q)dq}.$$

Finally, the adaptation law is given by

$$\dot{\hat{a}}_i = \Gamma(\dot{\hat{a}}_{pre_i} - I_{proj_i}\dot{\hat{a}}_{pre_i}), \tag{8}$$

with

$$\dot{\hat{a}}_{pre} = -F_i\hat{a}_i - \xi(\Lambda_i\hat{a}_i - \lambda_i) - \zeta \sum_{j\in\mathcal{N}_i}(\hat{a}_i - \hat{a}_j), \tag{9}$$

where $\xi, \zeta \in \mathbb{R}_+$ are scalar gains, $\Gamma \in \mathbb{R}^{m\times m}$ is a diagonal positive definite gain matrix. The variables F_i, Λ_i, and λ_i are given by the following equations,

$$F_i = \left[\int_{V_i} \mathcal{K}(q)(q - \hat{C}_{V_i})^T dq\right] \dot{p}_i \tag{10}$$

$$\Lambda_i = \int_0^t w(\tau)\mathcal{K}_i(\tau)\mathcal{K}_i(\tau)^T d\tau, \tag{11}$$

$$\lambda_i = \int_0^t w(\tau)\mathcal{K}_i(\tau)\phi_i(\tau)d\tau. \tag{12}$$

Given a set of indexed vertices $V_e = \{v_1 \ldots, v_n\}$ and a set of edges $E = \{e_1 \ldots e_l\}$, where $e_i = \{v_j, v_k\}$ then $\mathcal{N}_i = \{j|\{v_i, vj\} \in E\}$ *i.e.,* $\mathcal{N}_i$ contains the indexes of the vertices which are neighbors of the vertices associated to the Voronoi partition of the generator point i.

The matrix $I_{proj_i}(j)$ is defined as follows

$$I_{proj_i}(j) = \begin{cases} 0 & \text{for } \hat{a}_i(j) > \beta, \\ 0 & \text{for } \hat{a}_i(j) = \beta \text{ and } \dot{\hat{a}}_{pre_i} \geq 0, \\ 1 & \text{otherwise.} \end{cases} \tag{13}$$

The index j denotes the j-th diagonal element of the matrix I_{proj_i} and the j-th element of the vector $\hat{a}_i$. This matrix implements a projection law which prevents the parameter vector $\hat{a}_i$ from taking values less than or equal to the lower bound β.

The function $w(t) \in \mathcal{L}^1$ is called a weighting function we provide a detailed discussion in Section II-D.

Lastly, in [16] the authors state and prove the following convergence theorem

Theorem 1 (Convergence Theorem): Under Assumptions 1 and 2, for the system of n agents with the dynamics given by (6) and the control law in (7),

$$\lim_{t\to\infty} \|\hat{C}_{V_i} - p_i\| = 0, \ \forall i \in I_n,$$
$$\lim_{t\to\infty} \mathcal{K}(p_i(\tau))^T\tilde{a}_i = 0, \ \forall\tau \mid w(\tau) > 0 \text{ and } \forall i \in I_n,$$
$$\lim_{t\to\infty} \|\hat{a}_i - \hat{a}_j\| = 0, \ \forall i, j \in I_n,$$

with $I_n = \{1, \ldots, n\}$.

D. Weighting Functions

The weighting function $w(\cdot)$ in (11) and (12) should stimulate the parameter convergence of the adaptation law. Based on [16], if we choose $w(\tau)$ as a square wave, the integral given in (11) does not incorporate any other term in the summation after some fixed time determined by the decay time of the square wave. We can soften the elimination of old terms in the integral using softer decays, *e.g.,* an exponential decay $w(\tau) = e^{-\tau}$. If we specifically use the function $w(t, \tau) = e^{-\delta(t-\tau)}$ the integrals (11) and (12) become first-order systems, introducing a forgetting factor δ which allows the tracking of slow varying density functions.

III. Adaptive Control for Nonholonomic Sensors

The stability analyzes of the controllers in [13] and [16] have been conducted assuming holonomic kinematics, but now we propose to formally extend the previous results to nonholonomic vehicles.

A. Nonlinear Steering Control

In order to incorporate nonholonomic constrains in our model, we propose to use the polar unicycle model kinematics equations [20] for a differential steering as a suitable approach. The equations of motion for the i-th agent in the team of robots are given as follows

$$\begin{pmatrix} \dot{\rho}_i \\ \dot{\alpha}_i \\ \dot{\theta}_i \end{pmatrix} = \begin{pmatrix} -u_i\cos\alpha_i \\ -\omega_i + u_i\frac{\sin\alpha_i}{\rho_i} \\ u_i\frac{\sin\alpha_i}{\rho_i} \end{pmatrix}, \tag{14}$$

where

$$\alpha_i = \theta_i - \phi_i, \tag{15}$$
$$\dot{\phi}_i = \omega_i.$$

where u_i and ω_i are the linear and angular speeds of the i-th robot respectively.

After an extensive analysis of several controllers for nonholonomic systems available in the literature, the control algorithm described in [20] provided a suitable solution to our multivehicle coordination problem.

As shown in Fig. 1 the position of the agent inside its Voronoi cell is represented in polar coordinates where ϕ_i is the heading angle of the vehicle, ρ_i represents the position error between the agent and the centroid point and α_i is the angle between the principal axis of the robot and the vector error ρ_i. Now, the control law [20] is given by,

$$\begin{pmatrix} u_i \\ \omega_i \end{pmatrix} = \begin{pmatrix} (\gamma\cos\alpha_i)\rho_i \\ k\alpha_i + \gamma\frac{\cos\alpha_i\sin\alpha_i}{\alpha_i}(\alpha_i + h\theta_i) \end{pmatrix}, \tag{16}$$

where k, γ and h are positive gains.

The control law in (16) allows the agent to reach asymptotically the point $(0, 0, 0)$. Therefore if we carry out an axis translation to set the centroid at the origin of the plane we

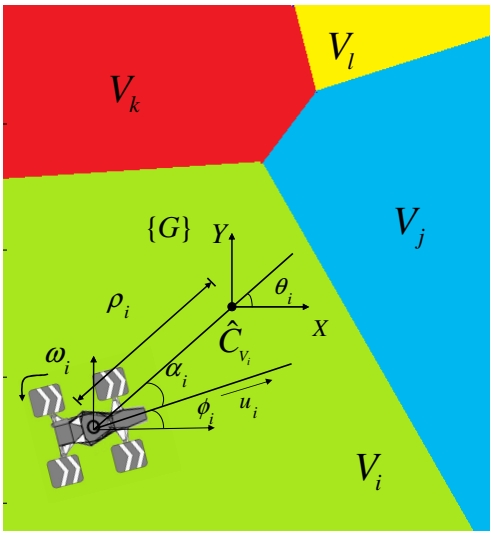

Fig. 1. Unicycle model and variables in the goal frame $\{G\}$: Notice the vectors and angles which determine our nonholonomic model in polar coordinates.

can use this control law to drive the robots to their centroidal Voronoi tessellation. For a detailed proof of the stability of the steering control (see [20]).

B. Stability Analysis

The following is our extended convergence theorem for the distributed and adaptive control for nonholonomic vehicles.

Theorem 2 (Extended Convergence Theorem): If Assumptions 1 and 2, are satisfied we have for the system of n nonholonomic agents with dynamics (14) and control law (16),

$$\begin{aligned}\lim_{t\to\infty} \mathcal{K}(p_i(\tau))^T\tilde{a}_i &= 0, \quad \forall\tau \mid w(\tau)>0 \text{ and } \forall i\in I_n,\\ \lim_{t\to\infty} \rho_i, \|\alpha_i\|, \|\theta_i\| &= 0, \quad \forall i\in I_n,\\ \lim_{t\to\infty} \|\hat{a}_i-\hat{a}_j\| &= 0, \quad \forall i,j\in I_n,\end{aligned}$$

with $I_n=\{1,\ldots,n\}$.

Proof: To carry out the stability analysis, we propose the following Lyapunov function candidate

$$V=\mathcal{H}+\sum_{i=1}^{n}\left[\frac{1}{2}\tilde{a}_i^T\Gamma^{-1}\tilde{a}_i+\frac{1}{2}\left(\alpha_i^2+h\theta_i^2\right)\right]. \tag{17}$$

The matrix Γ is the same diagonal positive definite matrix in (8), $\mathcal{H}$ is described by (1), and α_i, θ_i and ρ_i are the state variables in the dynamics in (14). Lastly, $\tilde{a}_i$ is the parameter estimation error given by (5).

Taking the time derivative of (17), we obtain

$$\dot{V}=\sum_{i=1}^{n}\left[\frac{\partial\mathcal{H}}{\partial p_i}\dot{p}_i+\tilde{a}_i^T\Gamma^{-1}\dot{\tilde{a}}_i+(\alpha\dot{\alpha}_i+h\theta_i\dot{\theta}_i)\right]. \tag{18}$$

Now, replacing (3) in (18) we get

$$\begin{aligned}\dot{V} &= \sum_{i=1}^{n}\Big[M_{V_i}(p_i-C_{V_i})^T\dot{p}_i+\tilde{a}_i^T\Gamma^{-1}\dot{\tilde{a}}_i\\ &\quad+(\alpha\dot{\alpha}_i+h\theta_i\dot{\theta}_i)\Big].\end{aligned} \tag{19}$$

Furthermore, we can show that

$$L_{V_i}=M_{V_i}\hat{C}_{V_i}+\tilde{M}_{V_i}(\hat{C}_{V_i}-\tilde{C}_{V_i})=M_{V_i}C_{V_i}, \tag{20}$$

then replacing (20) in (19), and taking into account that

$$\tilde{M}_{V_i}\tilde{C}_{V_i}-\tilde{M}_{V_i}\hat{C}_{V_i}=\tilde{a}_i\int_{V_i}\mathcal{K}(q)^T(q-\hat{C}_{V_i})dq,$$

as well as replacing the adaptation law given by (8)-(12) in (19), the final expression for the derivative of the Lyapunov function becomes

$$\begin{aligned}\dot{V} &= -\sum_{i=1}^{n}\Big[M_{V_i}(\hat{C}_{V_i}-p_i)^T\dot{p}_i\\ &\quad+\xi\int_0^t w(\tau)(\mathcal{K}_i(\tau)^T\tilde{a}_i)^2\,d\tau\\ &\quad+\tilde{a}_i^T\zeta\sum_{j\in N_i}(\hat{a}_i-\hat{a}_j)+\tilde{a}_i^T I_{proj}\dot{\hat{a}}_{pre_i}\\ &\quad-(\alpha_i\dot{\alpha}_i+h\theta_i\dot{\theta}_i)\Big].\end{aligned} \tag{21}$$

The second, third and fourth terms in the summation in (21) have already been proven to be positive semidefinite [16], considering the negative sign before the summation. Now, we are interested in proving that the first and fifth terms are positive semidefinite as well.

Calculating $\hat{C}_{V_i}-p_i$ and based on Fig. 1, we can assert that

$$\begin{aligned}\hat{C}_{V_i}-p_i &= \begin{pmatrix}x_2-x_1\\ y_2-y_1\end{pmatrix}=\begin{pmatrix}\rho_i\cos\theta_i\\ \rho_i\sin\theta_i\end{pmatrix}\\ &= \begin{pmatrix}\rho_i\cos(\phi_i+\alpha_i)\\ \rho_i\sin(\phi_i+\alpha_i)\end{pmatrix}.\end{aligned} \tag{22}$$

Taking the first term $M_{V_i}(\hat{C}_{V_i}-p_i)^T\dot{p}_i$ of (21) and replacing $\hat{C}_{V_i}-p_i$ and $\dot{p}_i$ by using the unicycle model in (14) with the control law in (16) we have

$$\begin{aligned}&M_{V_i}(\hat{C}_{V_i}-p_i)^T\dot{p}_i=\\ &= M_{V_i}\begin{pmatrix}\rho_i\cos(\phi_i+\alpha_i)\\ \rho_i\sin(\phi_i+\alpha_i)\end{pmatrix}^T\begin{pmatrix}(\gamma\cos\alpha_i)\rho_i\cos\phi_i\\ (\gamma\cos\alpha_i)\rho_i\sin\phi_i\end{pmatrix},\\ &= M_{V_i}\rho_i^2\gamma(\cos^2\phi_i\,\cos^2\alpha_i+\sin^2\phi_i\,\cos^2)\alpha_i,\\ &= M_{V_i}\rho_i^2\gamma\cos^2\alpha_i.\end{aligned} \tag{23}$$

Since the mass M_{V_i} of the i-th Voronoi region and the control gain γ are non-negative, the first term in the summation of (21) is non-negative.

$$M_{V_i}(\hat{C}_{V_i}-p_i)^T\dot{p}_i=M_{V_i}\rho_i^2\gamma\cos^2\alpha\geq 0.$$

Analyzing the fifth term in (21) we have that based on [20], if we replace the polar kinematics in (14) and replace the control law given by (16) in $-(\alpha_i\dot{\alpha}_i+h\theta_i\dot{\theta}_i)$ we get

$$-(\alpha_i\dot{\alpha}_i+h\theta_i\dot{\theta}_i)=k\alpha_i^2\geq 0,$$

and the fifth term $-(\alpha_i\dot{\alpha}_i+h\theta_i\dot{\theta}_i)$ in (21) is non-negative. Since V is lower bounded, $\dot{V}$ is negative semidefinite and uniformly continuous in time, we conclude that $\dot{V}\to 0$ as $t\to\infty$ by the Lyapunov-like lemma.

From the Lyapunov function derivative in (21) it is easy to see that all the limits converge to zero except the third one $\lim_{t\to\infty}\|\theta_i(t)\|$. In [20] the author proved by the Lyapunov-like lemma that $\dot{\alpha}_i \to 0$ as $t \to \infty$ and this implies that $\theta_i \to 0$ as well. Therefore the controller guarantees the convergence of the state variables ρ_i, α_i and θ_i to zero under the goal frame $\{G\}$ shown in Fig. 1. ■

Remark 1: Although the orientation of the robot with repect to the global frame is a consequence of the nonlinear steering control, it can be required to regulate the orientation of the mobile sensor since a robot can have navigation sensors such as a camera or laser range finder at the front part.

Remark 2: From (14) and (16) we have singularities when $\rho_i = 0$ or $\alpha_i = 0$. this singularities are an issue from the theoretical point of view, but in a practical application they can be addressed by forcing the car to stop when the car is located within certain minimum distance $\rho_i \neq 0$ or minimum angle $\alpha_i \neq 0$ such that the singularity is never reached.

C. Dynamic Density Function

We consider the case of estimating the parameters of a time-varying density function $\phi_i(q,t) = \mathcal{K}(q)^T a(t)$ where the j-th entry $a_j(t)$ $(j = 1, 2, \ldots, m)$ of $a(t)$ is a piecewise constant function $a_j(t) : \mathbb{R}^m_+ \mapsto \mathbb{R}^m_+$ and is right continuous. It means that every entry of the function vector $a(t)$ has a finite number of discontinuities and takes on constant values between two consecutive discontinuities. This is a reasonable approximation if we consider slow-time varying systems. Also, we assume that $\lim_{t\to\infty} a(t) = a_c$ where $a_c \in \mathbb{R}^m_+$ is a constant value *i.e.,* the density function reaches a steady state which is reasonable for many real-world phenomena such as oil spills [1] and forest fires [2].

From now on, we will call *switching time* t_s, the time when each discontinuity happens, where $s = 1, \cdots, k$, and k is the total number of switching times before the density function reaches its final value. This terminology was taken from [21] given the partial similarity with the switching systems. Moreover let us assume that the adaptation law rate and the angular and linear speeds of the agents are fast enough to follow the dynamics of the density function $\phi(q,t)$.

From (8) we know that every robot looks for the centroid of its Voronoi cell while taking measurements of the distribution function on its trajectory. During this time, the tracking error decreases but notice from Theorem 2 that the network of robots converges to a near optimal coverage configuration. Based on Theorem 2 this behavior does not necessarily imply that the parameter estimation vector $\tilde{a}(t) \to 0$ as $t \to \infty$.

Furthermore, since we are dealing with a piecewise constant system, the time interval between two switching times $\Delta t_s = t_s - t_{s-1}$ is finite, in contrast with the infinite time necessary to guarantee full parameter convergence.

IV. Simulations

For this simulation we used a population of 20 unicycle models randomly distributed over a sample space Q defined as a unit square. We implement the control law given in (16) with $\gamma = 3$ and $k = h = 1$. The parameter values we used in the adaptation law given by (8) and (9) are $\Gamma = I_{64}$, $\xi = 1000$, $\zeta = 1$ and $\delta = 1$. For the matrix I_{proj_i} defined by (13), we have $\beta = 0.1$. The simulation parameters were calculated by extensive numerical simulations.

We divided the sampling space Q in a 8×8 grid where the geometric center of every square cell corresponds to the mean μ_i of a bidimensional Gaussian function. Using a function similar to the one in [16] we have that the i-th entry $\mathcal{K}_i$ of the vector function $\mathcal{K}(q)_{64\times 1}$ is calculated as,

$$\mathcal{K}_i = e^{\frac{-(q-\mu_i)^2}{2\sigma_i^2}}, \tag{24}$$

with $\sigma_i^2 = 0.05$.

For this simulation we use the team of robots to detect a density function which behaves as an expanding circle. The circle recreates a simplified behavior of a forest fire where the higher temperatures are localized at the boundary of the circle.

The dynamics of the expanding circle are modeled by the following parametric equations,

$$\begin{pmatrix} x(t) \\ y(t) \end{pmatrix} = c_1 r(t) \begin{pmatrix} \cos\phi \\ \sin\phi \end{pmatrix} + \begin{pmatrix} c_2 \\ c_3 \end{pmatrix},$$

with the radius $r(t)$ defined by the differential equation,

$$\dot{r}(t) = -c_4 r(t) + c_5,$$

with the constants $r(0) \in \mathbb{R}^+$ and $c_i \in \mathbb{R}_+$ for $i = 1, 2 \ldots 5$.

In order to assign a height to the expanding circle, we take m equidistant points at the boundary of the circle. Each point determines the mean of a bidimensional gaussian function with variance $\sigma_k^2 = 0.05$ which is sampled by the 8×8 grid defined above in Q. The heights of each one of the 64 samples determine the parameter vector $a(t)$. In Fig. 2 we show a simplified 1-dimensional version of this calculation where the red dots labeled P_1 and P_2 are equivalent to the m dots in the boundary of the circle. The gaussian functions are indicated in red and assuming we discretized the space in 8 bins we sample the gaussians so that we get the eight parameters $a_i(t)$ with $i = 1, 2 \ldots 8$ as shown in Fig. 2.

Since our approach covers just piecewise constant dynamics we assume that the robots are taking measurements of the density function at the discrete-time instants 0, 20, 40 and 100 s. This means that assuming a slow varying distribution function the robots can reach their respective centroids and rest until some problem dependent condition is fulfilled to start taking measurements again.

1) Simulation Results in Matlab: In Fig. 3 we show the averaged behavior of the parameter estimation error given by

$$\mathcal{K}(p_i(\tau))^T \tilde{a}_i(t) \ \forall\tau \ |w(\tau) > 0,$$

as well as the error distance $\rho_i(t)$, the angle $\alpha_i(t)$ and the consensus error given by

$$\|\hat{a}_i(t) - \hat{a}_j(t)\| \ \forall i, j \in I_n.$$

Notice that the switching times of the simulation are indicated by the dashed vertical lines in green.

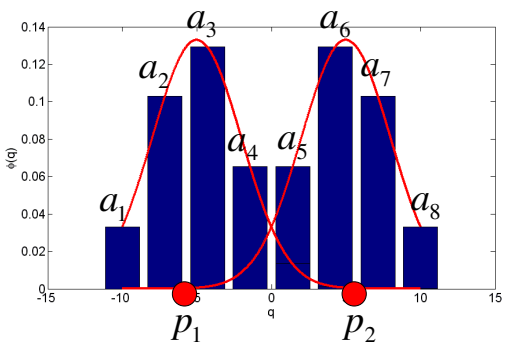

Fig. 2. Method to create the parametric density function. The two red dots at p_1 and p_2 determine the two gaussians which are sampled to determine the parameters $a_i(t)$ for $i = 1, 2 \ldots 8$.

Let us define

$$\bar{\tilde{a}}_i(t) = \frac{1}{n}\left(\sum_{i=1}^{n} \tilde{a}_i(t)\right) \quad \forall t > 0, \tag{25}$$

which is the averaged parameter error vector over all robots. In Fig. 3 (a) we show the parameter estimation error $\mathcal{K}(q)^T \bar{\tilde{a}}_i(t)$ averaged over the whole population of robots. In a similar way let us define

$$\bar{\rho}(t) = \frac{1}{n}\left(\sum_{i=1}^{n} \rho_i(t)\right) \quad \forall t > 0, \tag{26}$$

which is the averaged position error of all the robots in Q, which is plotted in Fig. 3 (b).

Finally, for the consensus error let us define the quantity c_a as

$$c_a = \sum_{i=1}^{n} \left\| \sum_{j=1}^{n} (\hat{a}_i - \hat{a}_j) \right\|^2, \tag{27}$$

which shows the summation of the squared norm of the vector $\sum_{j=1}^{n}(\hat{a}_i - \hat{a}_j)$ over the whole population of robots and is plotted in Fig. 3 (d).

In the plots in Fig. 3 (a), (c) and (d) it is easy to note the asymptotic convergence to zero after every switching time t_s, but in the case of α_i this is difficult to see because the approximation of the numerical integrals of the centroids in (2) induces some noise in the trajectory of the robots. Furthermore, notice that the transitions of α_i from $-\pi$ to π look like spikes in the plot, however, the robots spend the majority of the time oscillating around the angle $\alpha_i = 0$ as the filtered red signal illustrates in Fig. 3 (b).

V. Experimental Verification

The experiments were carried out using a population of four P3-AT robots, sensing a white light concentration in a rectangular sampling space of 4.7×6.6 m. The sampling

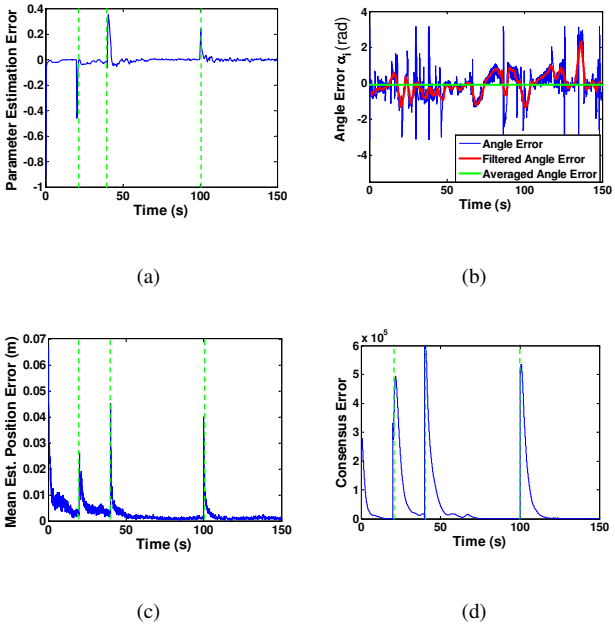

Fig. 3. Plots of the parameter estimation error $\mathcal{K}(q)^T \bar{\tilde{a}}_i(t)$, the error distance $\bar{\rho}(t)$, the angle α_i and the consensus error c_a for the simulation.

space was divided into a 8×8 grid. The geometric center of each rectangular division corresponds to the mean of a bidimensional Gaussian function given by (24) with $\sigma_i^2 = 0.7$ m.

The adaptation law is a differential equation, which is not suitable for real-time applications. Instead, we used the following approximations of (9), (11) and (12), based on [22]

$$\lambda_i(t+1) = \lambda_i(t) + \mathcal{K}(p_i(t))\phi_i(t), \tag{28}$$

$$\Lambda_i(t+1) = \Lambda_i(t) + \mathcal{K}(p_i(t))\mathcal{K}(p_i(t))^T, \tag{29}$$

$$\hat{a}_{i_{pre}} = \hat{a}_i + \xi(\Lambda_i \hat{a}_i - \lambda_i) - \zeta \sum_{j \in \mathcal{N}_i} (\hat{a}_i - \hat{a}_j) \tag{30}$$

$$\hat{a}_i = \max(\hat{a}_{i_{pre}}, \beta). \tag{31}$$

were used in order to carry out the adaptation law calculation in real time. The parameter values we used in the approximation of the adaptation law given by (28) – (31) are $\xi = 1000$, $\zeta = 1$ and $\delta = 1$. The matrix I_{proj_i} defined by (13) now is replaced by the max operation in (31) $\beta = 0.1$. The experiment parameters were determined by trial and error.

The light concentration is dynamic under the assumptions presented in Section III-C. There is one switching time t_s to switch between two different light sources at 108 s of the experiment. The wheel encoders embedded in the robots are used for relative robot positioning. A set of four Phidgets light precision sensors [23] are set up at the top of the robots and the network communication with the robots is carried out using Player 3.0.0 [24] through a Linksys wireless router.

A. Experimental Results

In Fig. 4 (a) and (b) we show the behavior of the error distance $\bar{\rho}(t)$ defined in (26), and the consensus error c_a

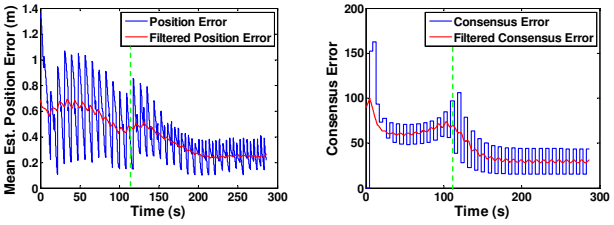

(a) (b)

Fig. 4. Plots of the error distance $\bar{\rho}(t)$ and the consensus error c_a for the experiments.

given by (27). Notice the convergence of the signal in Fig. 4 (a) and (b) which are visibly affected by the noise of the real measurements and the numeric approximation of the centroid integrals. In order to make them clear, we plot the filtered signal in red. Furthermore, the approximation of the adaptive law given by (31) induces additional noise on the plots. More details about the hardware implementation are available in [25]. The reader can find videos about the simulation and experimental results at `http://controls.ece.unm.edu/index.php/CDC_2010_Video`.

VI. Conclusions

We have developed an adaptive controller for deployment of nonholonomic sensor networks to carry out a coverage and estimation of a parameterizable density function in a convex sampling space. We provided a stability theorem which states that the robots distribute themselves in an optimal way over the density function solving the locational optimization problem. The mobile sensors were modeled as unicycle vehicles, and a nonlinear steering control law in polar coordinates was used to drive them and guarantee stability. Through simulations in Matlab, we verified our theoretical results. Some experiments using a team of four P3-AT robots explains the gap between theory and practice. However, the theoretical results still work since the system curves exhibit the convergence stated by Theorem 2. The theoretical extension of the problem to a continuous time-varying density function rather than piece-wise constant function, as well as the reduction of the noise effect in the experimental results, are part of our future research agenda.

VII. Acknowledgments

The work was supported by DOE URPR (University Research Program in Robotics) grant DE-FG52-04NA25590 and by NSF grants ECCS CAREER #0811347, IIS #0812338, and CNS #0709329.

References

[1] J. Clark and R. Fierro, "Mobile robotic sensors for perimeter detection and tracking," *ISA Trans.*, vol. 45, pp. 3–13, 2007.

[2] D. W. Casbeer, D. B. Kingston, R. W. Beard, T. W. Mclain, S. M. Li, and R. Mehra, "Cooperative forest fire surveillance using a team of small unmanned air vehicles," *International Journal of Systems Sciences*, vol. 37, no. 6, pp. 351–360, 2006.

[3] R. A. Cortez, "Information-driven cooperative control for radiation map building," M.S. Thesis, The University of New Mexico, 2007.

[4] H. Choset, "Coverage for robotics – a survey of recent results," *Annals of Mathematics and Artificial Intelligence*, vol. 31, no. 1-4, pp. 113–126, 2001.

[5] R. A. Cortez and H. G. Tanner, "Radiation mapping using multiple robots," in *2nd ANS International Joint Topical Meeting on Emergency Preparedness & Response and Robotic & Remote Systems*, March 2008.

[6] P. Ögren, E. Fiorelli, and N. E. Leonard, "Cooperative control of mobile sensor networks: Adaptive gradient climbing in a distributed environment," *IEEE Transactions on Automatic Control*, vol. 8, no. 49, pp. 1292 – 1302, 2004.

[7] M. Pavone, A. Arsie, E. Frazzoli, and F. Bullo, "Equitable partitioning policies for robotic networks," in *Proc. of the International Conference on Robotics and Automation (ICRA 09)*, Kobe, Japan, May 2009, pp. 2356–2361.

[8] J. G. M. Fu, T. Bandyopadhyay, and M. H. A. Jr, "Local voronoi decomposition for multi-agent task allocation," in *Proc. of the International Conference on Robotics and Automation (ICRA 09)*, Kobe, Japan, May 12-17 2009, pp. 1935–1940.

[9] J. Stergiopoulos and A. Tzes, "Voronoi-based coverage optimization for mobile networks with limited sensing range a directional search approach," in *Proc. of the American Control Conference (ACC 09)*, St. Louis, Missouri, Jun 10-12 2009, pp. 2642–2647.

[10] A. Deshpande, S. Poduri, D. Rus, and G. S. Sukhatme, "Distributed coverage control for mobile sensors with location-dependent sensing models," in *Proc. of the International Conference on Robotics and Automation (ICRA 09)*, Kobe, Japan, May 2009, pp. 2344–2349.

[11] G. Lee, N. Chong, and H. Christensen, "Adaptive triangular mesh generation of self-configuring robot swarms," in *Proc. of the International Conference on Robotics and Automation (ICRA 09)*, Kobe, Japan, May 2009, pp. 2737–2742.

[12] M. Schwager, B. J. Julian, and D. Rus, "Optimal coverage for multiple hovering robots with downward facing cameras," in *Proc. of the International Conference on Robotics and Automation (ICRA 09)*, Kobe, Japan, May 12-17 2009, pp. 3515–3522.

[13] J. Cortés, S. Martínez, T. Karatas, and F. Bullo, "Coverage control for mobile sensing networks," *IEEE Transactions on robotics and Automation*, vol. 20, pp. 243–255, 2004.

[14] M. Franceschelli, M. Egerstedt, A. Giua, and C. Mahulea, "Constrained invariant motions for networked multi-agent systems," in *Proc. of the International Conference on Robotics and Automation (ICRA 09)*, Kobe, Japan, May 12-17 2009, pp. 5749–5754.

[15] A. Kwok and S. Martínez, "Unicycle coverage control via hybrid modeling," *IEEE Transactions on Automatic Control*, submitted, 2008, revised 2009.

[16] M. Schwager, D. Rus, and J. J. E. Slotine, "Decentralized, adaptive control for coverage with networked robots," *International Journal of Robotics Research*, vol. 28, no. 3, pp. 357–375, March 2009.

[17] "Voro++ documentation," [online] Available: http://math.lbl.gov/voro++/doc/, 2009.

[18] Q. Du and M. Gunzburguer, "Centroidal voronoi tessellations: Applications and algorithms," *SIAM Review*, vol. 41, pp. 637–676, 1999.

[19] F. Bullo, J. Cortés, and S. Martínez, *Distributed Control of Robotic Networks*, ser. Applied Mathematics Series, 2009, available at http://www.coordinationbook.info.

[20] G. Casalino, M. Aicardi, A. Bicchi, and A. Balestrino, "Closed loop steering and path following for unicycle-like vehicles: a simple lyapunov function based approach," *IEEE Robotics and Automation Magazine*, vol. 2, no. 1, pp. 27–35, March 1995.

[21] D. Liberzon, *Switching in Systems and Control*, ser. Systems & Control: Foundations & Applications, Birkhauser, Ed., June 2003.

[22] M. Schwager, J. McLurkin, J. J. E. Slotine, and D. Rus, "From theory to practice: Distributed coverage control experiments with groups of robots," in *Proceedings of the International Symposium on Experimental Robotics*, Athens, Greece, July 2008.

[23] "Product manual. 1127 - precision light sensor," [online] Available: http://www.phidgets.com/documentation/Phidgets/1127.pdf, 2007.

[24] "The player robot device interface," [online] Available: http://playerstage.sourceforge.net/doc/Player-2.1.0/player/index.html, 2007.

[25] R. A. Cortez, , J. M. Luna, R. Fierro, and J. Wood, "Multi-vehicle testbed for decentralized environmental sensing," in *Proc. of the IEEE International Conference on Robotics and Automation (ICRA 2010)*, Anchorage, Alaska, May 2010.